LETTER

doi:10.1038/nature10201

A low mass for Mars from Jupiter's early gas-driven migration

Kevin J. Walsh[1,2], Alessandro Morbidelli[1], Sean N. Raymond[3,4], David P. O'Brien[5] & Avi M. Mandell[6]

Jupiter and Saturn formed in a few million years (ref. 1) from a gas-dominated protoplanetary disk, and were susceptible to gas-driven migration of their orbits on timescales of only ~100,000 years (ref. 2). Hydrodynamic simulations show that these giant planets can undergo a two-stage, inward-then-outward, migration[3–5]. The terrestrial planets finished accreting much later[6], and their characteristics, including Mars' small mass, are best reproduced by starting from a planetesimal disk with an outer edge at about one astronomical unit from the Sun[7,8] (1 AU is the Earth–Sun distance). Here we report simulations of the early Solar System that show how the inward migration of Jupiter to 1.5 AU, and its subsequent outward migration, lead to a planetesimal disk truncated at 1 AU; the terrestrial planets then form from this disk over the next 30–50 million years, with an Earth/Mars mass ratio consistent with observations. Scattering by Jupiter initially empties but then repopulates the asteroid belt, with inner-belt bodies originating between 1 and 3 AU and outer-belt bodies originating between and beyond the giant planets. This explains the significant compositional differences across the asteroid belt. The key aspect missing from previous models of terrestrial planet formation is the substantial radial migration of the giant planets, which suggests that their behaviour is more similar to that inferred for extrasolar planets than previously thought.

Hydrodynamic simulations show that isolated giant planets embedded in gaseous protoplanetary disks carve annular gaps and migrate inward[9]. Saturn migrates faster than Jupiter; if Saturn is caught in the 2:3 mean motion resonance with Jupiter (conditions for this to happen are given in Supplementary Information section 3), where their orbital period ratio is 3/2, generally the two planets start to migrate outward until the disappearance of the disk[3–5,10]. Jupiter could have migrated inward only before Saturn approached its final mass and was captured in resonance. The extents of the inward and outward migrations are unknown a priori owing to uncertainties in disk properties and in relative timescales for the growth of Jupiter and Saturn. Thus we search for constraints on where Jupiter's migration may have reversed (or 'tacked', using a sailing analogy).

The terrestrial planets are best reproduced when the disk of planetesimals from which they form is truncated, with an outer edge at 1 AU (refs 7, 8). These conditions are created naturally if Jupiter tacked at ~1.5 AU. However, before concluding that Jupiter tacked at this distance, a major question needs to be addressed: can the asteroid belt, between 2 and 3.2 AU, survive the passage of Jupiter?

Volatile-poor asteroids (mostly S types) are predominant in the inner asteroid belt, while volatile-rich asteroids (mostly C types) are predominant in the outer belt. These two main classes of asteroids have partially overlapping semimajor axis distributions[11,12], though C types outnumber S types beyond ~2.8 AU. We ran a suite of dynamical simulations to investigate whether this giant planet migration scheme is consistent with the existence and structure of the asteroid belt. Because of the many unknowns in giant planet growth and early dynamical evolution, we present a simple scenario that reflects one plausible history for the giant planets (Fig. 1). We provide an exploration of parameter space (see Supplementary Information) that embraces a large range of possibilities and demonstrates the robustness of the results. In all simulations, we maintain the fundamental assumption that Jupiter tacked at 1.5 AU.

Figure 2 shows how the migration of the giant planets affects the small bodies. The disk interior to Jupiter has a mass 3.7 times that of the Earth ($3.7M_{\oplus}$), equally distributed between planetary embryos (large)

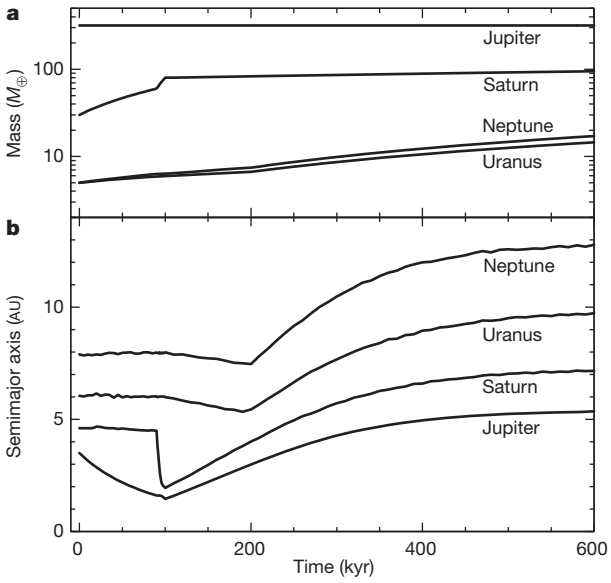

Figure 1 | The radial migration and mass growth imposed on the giant planets in the reference simulation. a, Mass growth; **b**, semimajor axis. A fully-formed Jupiter starts at 3.5 AU, a location expected to be highly favourable for giant planet formation owing to the presence of the so-called snow line[21]. Saturn's 30 $M_{\oplus}$ core is initially at ~4.5 AU and grows to 60 $M_{\oplus}$ as Jupiter migrates inward, over 10^5 years. Inward type-I migration of planetary cores is inhibited in disks with a realistic cooling timescale[23–26]; thus Saturn's core remains at 4.5 AU during this phase. Similarly, the cores of Uranus and Neptune begin at ~6 and 8 AU and grow from 5 $M_{\oplus}$, without migrating. Once Saturn reaches 60 $M_{\oplus}$ its inward migration begins[25], and is much faster than that of the fully grown Jupiter[27]. Thus, on catching Jupiter, Saturn is trapped in the 2:3 resonance[3]. Here this happens when Jupiter is at 1.5 AU. The direction of migration is then reversed, and the giant planets migrate outward together. In passing, they capture Uranus and Neptune in resonance and these planets are then pushed outwards as well. Saturn, Uranus and Neptune reach their full mass at the end of the migration when Jupiter reaches 5.4 AU. The migration rate decreases exponentially as the gas disk dissipates. The final orbital configuration of the giant planets is consistent with their current orbital configuration when their later dynamical evolution is considered[28,29] (see Supplementary Information section 3 for extended discussion).

[1]Université de Nice – Sophia Antipolis, CNRS, Observatoire de la Côte d'Azur, BP 4229, 06304 Nice Cedex 4, France. [2]Department of Space Studies, Southwest Research Institute, 1050 Walnut Street, Suite 300, Boulder, Colorado 80302, USA. [3]Université de Bordeaux, Observatoire Aquitain des Sciences de l'Univers, 2 Rue de l'Observatoire, BP 89, F-33270 Floirac Cedex, France. [4]CNRS, UMR 5804, Laboratoire d'Astrophysique de Bordeaux, 2 Rue de l'Observatoire, BP 89, F-33270 Floirac Cedex, France. [5]Planetary Science Institute, 1700 East Fort Lowell, Suite 106, Tucson, Arizona 85719, USA. [6]NASA Goddard Space Flight Center, Code 693, Greenbelt, Maryland 20771, USA.

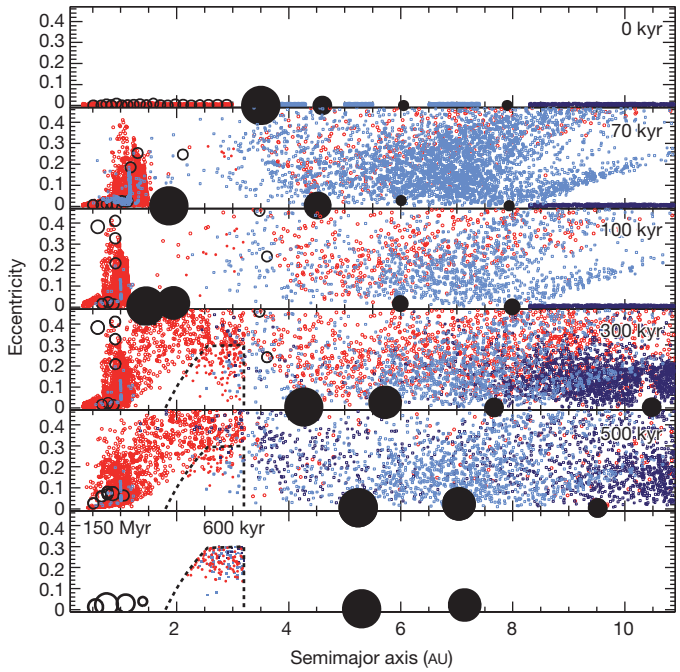

Figure 2 | The evolution of the small-body populations during the growth and migration of the giant planets, as described in Fig. 1. Jupiter, Saturn, Uranus and Neptune are represented by large black filled circles with evident inward-then-outward migration, and evident growth of Saturn, Uranus and Neptune. S-type planetesimals are represented by red dots, initially located between 0.3 and 3.0 AU. Planetary embryos are represented by large open circles scaled by $M^{1/3}$ (but not in scale relative to the giant planets), where M is mass. The C-type planetesimals starting between the giant planets are shown as light blue dots, and the outer-disk planetesimals as dark blue dots, initially between 8.0 and 13.0 AU. For all planetesimals, filled dots are used if they are inside the main asteroid belt and smaller open dots otherwise. The approximate boundaries of the main belt are drawn with dashed curves. The bottom panel combines the end state of the giant planet migration simulation (including only those planetesimals that finish in the asteroid belt) with the results of simulations of inner disk material (semimajor axis $a < 2$) evolved for 150 Myr (see Fig. 4), reproducing successful terrestrial planet simulations[8].

and planetesimals (small), while the planetesimal population exterior to Jupiter is partitioned between inter-planetary belts and a trans-Neptunian disk (8–13 AU). The planetesimals from the inner disk are considered to be 'S type' and those from the outer regions 'C type'. The computation of gas drag assumes 100-km-diameter planetesimals and uses a radial gas density profile taken directly from hydrodynamic simulations[4] (see Supplementary Information for details).

The inward migration of the giant planets shepherds much of the S-type material inward by resonant trapping, eccentricity excitation and gas drag. The mass of the disk inside 1 AU doubles, reaching $\sim 2M_{\oplus}$. This reshaped inner disk constitutes the initial condition for terrestrial planet formation. However, a fraction of the inner disk (~14%) is scattered outward, ending up beyond 3 AU. During the subsequent outward migration of the giant planets, this scattered disk of S-type material is encountered again. Of this material, a small fraction (~0.5%) is scattered inward and left decoupled from Jupiter in the asteroid belt region as the planets migrate away. The giant planets then encounter the material in the Jupiter–Neptune formation region, some of which (~0.5%) is also scattered into the asteroid belt. Finally, the giant planets encounter the disk of material beyond Neptune (within 13 AU) of which only ~0.025% reaches a final orbit in the asteroid belt. When the giant planets have finished their migration, the asteroid belt population is in place, whereas the terrestrial planets require an additional ~30 Myr to complete their accretion.

The asteroid belt implanted in the simulations is composed of two separate populations: the S-type bodies originally from within 3.0 AU, and the C types from between the giant planets and from 8.0 to 13.0 AU. The present-day asteroid belt consists of more than just S- and C-type asteroids, but this diversity is expected to result from compositional gradients within each parent population (Supplementary Information). There is a correlation between the initial and final locations of implanted asteroids (Fig. 3a). Thus, S-type objects dominate in the inner belt, while C-type objects dominate in the outer belt (Fig. 3b). Both types of asteroid share similar distributions of eccentricity and inclination (Fig. 3c, d). The present-day asteroid belt is expected to have had its eccentricities and inclinations reshuffled during the so-called late heavy bombardment (LHB)[13,14]; the final orbital distribution in our simulations matches the conditions required by LHB models.

Given the overall efficiency of implantation of ~0.07%, our model yields $\sim 1.3 \times 10^{-3}\ M_{\oplus}$ of S-type asteroids at the time of the dissipation of the solar nebula. In the subsequent 4.5 Gyr, this population will be depleted by 50–90% during the LHB event[13,14] and by a further factor of ~2–3 by chaotic diffusion[15]. The present-day asteroid belt is estimated to have a mass of $6 \times 10^{-4}\ M_{\oplus}$, of which 1/4 is S-type and 3/4 is C-type[12]. Thus our result is consistent within a factor of a few with the S-type portion of the asteroid belt.

The C-type share of the asteroid belt is determined by the total mass of planetesimals between the giant planets and between 8 and 13 AU, which are not known a priori. Requiring that the mass of implanted C-type material be three times that of the S-type, and given the implantation efficiencies reported above, this implies that the following

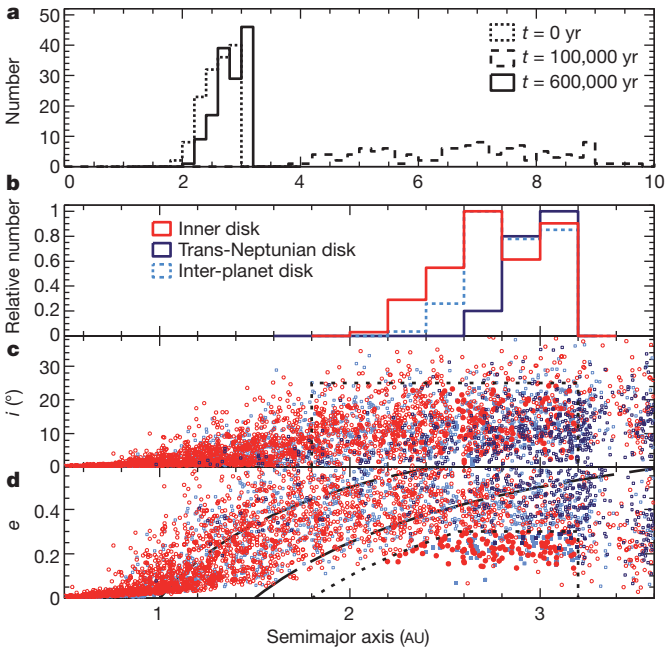

Figure 3 | Distributions of 100-km planetesimals at the end of giant planet migration. a, The semimajor axis distribution for the bodies of the inner disk that are implanted in the asteroid belt are plotted at three times: the beginning of the simulation (dotted histogram), at the end of inward planet migration (dashed) and at the end of outward migration (solid). There is a tendency for S-type planetesimals to be implanted near their original location. Thus, the outer edge of their final distribution is related to the original outer edge of the S-type disk, which in turn is related to the initial location of Jupiter. **b**, The final relative numbers of the S-type (red histogram), the inter-planet population (light blue) and the outer-disk (dark blue) planetesimals that are implanted in the asteroid belt are shown as a function of semimajor axis. The orbital inclination (**c**) and eccentricity (**d**) are plotted as a function of semimajor axis, with the same symbols used in Fig. 2. The dotted lines show the extent of the asteroid belt region for both inclination and eccentricity, and the dashed lines show the limits for perihelion less than 1.0 (left line) and 1.5 (right line). Most of the outer-disk material on planet-crossing orbits has high eccentricity, while many of the objects from between the giant planets were scattered earlier and therefore damped to lower-eccentricity planet-crossing orbits.

amount of material is left over from the giant planet accretion process: $\sim 0.8\ M_\oplus$ of material between the giant planets; $\sim 16\ M_\oplus$ of planetesimals from the 8.0–13 AU region; or some combination of the two.

Our simulations also found C-type material placed onto orbits crossing the still-forming terrestrial planets. For every C-type planetesimal from beyond 8 AU that was implanted in the outer asteroid belt, 11–28 C-type planetesimals ended up on high-eccentricity orbits that enter the terrestrial-planet-forming region (with perihelion $q < 1.0$–1.5 AU; see Fig. 3), and may represent a source of water for Earth[16]. For the Jupiter–Uranus region this ratio is 15–20, and for the Uranus–Neptune region it is 8–15. Thus, depending on which region dominated the implantation of C-type asteroids, we expect that $(3-11)\times 10^{-2}\ M_\oplus$ of C-type material entered the terrestrial planet region. This exceeds by a factor of 6–22 the minimal mass required to bring the current amount of water to the Earth ($\sim 5\times 10^{-4}\ M_\oplus$; ref. 17), assuming that C-type planetesimals are 10% water by mass[18].

We now consider the terrestrial planets. The migration of Jupiter creates a truncated inner disk matching initial conditions of previously successful simulations of terrestrial planet formation[8], though there is a slight build-up of dynamically excited planetary embryos at 1.0 AU. Thus, we ran simulations of the accretion of the surviving objects for 150 Myr. Earth and Venus grow within the 0.7–1 AU annulus, accreting most of the mass, while Mars is formed from embryos scattered out beyond the edge of the truncated disk. Our final distribution of planet mass versus distance quantitatively reproduces the large mass ratio existing between Earth and Mars, and also matches quantitative metrics of orbital excitation (Fig. 4).

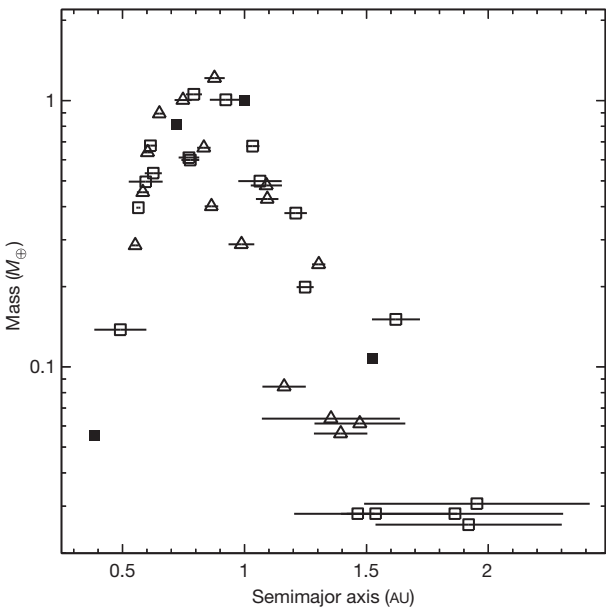

Figure 4 | Results of the eight terrestrial planet simulations. The mass versus semimajor axis of the synthetic planets (open symbols) is compared to the real planets (filled squares). The triangles refer to simulations starting with 40 embryos of $\sim 0.051\ M_\oplus$, and squares to simulations from 80 embryos of $\sim 0.026\ M_\oplus$. The horizontal error bars show the perihelion–aphelion excursion of each planet along their orbits. The initial planetesimal disk had an inner edge at 0.7 AU to replicate previous work[8], and an outer edge at $\sim$1.0 AU owing to the truncation caused by the inward and outward migration of the giant planets as described in the text. Half of the original mass of the disk interior to Jupiter ($1.85 M_\oplus$) was in $\sim$727 planetesimals. At the end of giant planet migration, the evolution of all objects inward of 2 AU was continued for 150 Myr, still accounting for the influence from Jupiter and Saturn. Collisions of embryos with each other and with planetesimals were assumed fully accretional. For this set of eight simulations, the average normalized angular momentum deficit[30] was 0.0011 ± 0.0006, as compared to 0.0018 for the current Solar System. Similarly, the radial mass concentration[30] was 83.8 ± 12.8 as compared to 89.9 for the current Solar System.

Similar qualitative and quantitative results were found for a number of migration schemes, a range of migration and gas disk dissipation timescales, and a range of gas density and planetesimal sizes (all described in Supplementary Information). Our results represent a major shift in the understanding of the early evolution of the inner Solar System. In our scheme, C-type asteroids form between and beyond the giant planets, nearer to comets than to S-type asteroids. This could explain the substantial physical differences between S-type and C-type asteroids, and also the physical similarities between the latter and comets (as shown by the Stardust mission and micrometeorite samples[19,20]; see Supplementary Information for more on physical properties).

If Jupiter and Saturn have migrated substantially, then their birth region could have been closer to the estimated location of the snow line (the expected condensation front for water) at $\sim$3 AU (ref. 21), rather than out beyond 5 AU. Also, substantial migration is a point of similarity with observed extrasolar planetary systems, in which migration is seemingly ubiquitous—extrasolar giant planets are commonly found at $\sim$1.5 AU (refs 2, 22). However, a difference between our Solar System and the currently known extrasolar systems is that, according to our results, Jupiter 'tacked' at 1.5 AU and then migrated outward, owing to the presence of Saturn.

Received 1 September 2010; accepted 1 April 2011.
Published online 5 June 2011.

1. Haisch, K. E. Jr, Lada, E. A. & Lada, C. J. Disk frequencies and lifetimes in young clusters. *Astrophys. J.* **553,** L153–L156 (2001).
2. Armitage, P. J. Massive planet migration: theoretical predictions and comparison with observations. *Astrophys. J.* **665,** 1381–1390 (2007).
3. Masset, F. & Snellgrove, M. Reversing type II migration: resonance trapping of a lighter giant protoplanet. *Mon. Not. R. Astron. Soc.* **320,** L55–L59 (2001).
4. Morbidelli, A. & Crida, A. The dynamics of Jupiter and Saturn in the gaseous protoplanetary disk. *Icarus* **191,** 158–171 (2007).
5. Pierens, A. & Nelson, R. P. Constraints on resonant-trapping for two planets embedded in a protoplanetary disc. *Astron. Astrophys.* **482,** 333–340 (2008).
6. Kleine, T. *et al.* Hf-W chronology of the accretion and early evolution of asteroids and terrestrial planets. *Geochim. Cosmochim. Acta* **73,** 5150–5188 (2009).
7. Wetherill, G. W. in *Protostars and Planets* (ed. Gehrels, T.) 565–598 (IAU Colloquium 52, International Astronomical Union, 1978).
8. Hansen, B. M. S. Formation of the terrestrial planets from a narrow annulus. *Astrophys. J.* **703,** 1131–1140 (2009).
9. Lin, D. N. C. & Papaloizou, J. On the tidal interaction between protoplanets and the protoplanetary disk. III — Orbital migration of protoplanets. *Astrophys. J.* **309,** 846–857 (1986).
10. Crida, A. Minimum mass solar nebulae and planetary migration. *Astrophys. J.* **698,** 606–614 (2009).
11. Gradie, J. & Tedesco, E. Compositional structure of the asteroid belt. *Science* **216,** 1405–1407 (1982).
12. Mothé-Diniz, T., Carvano, J. M., Á. & Lazzaro, D. Distribution of taxonomic classes in the main belt of asteroids. *Icarus* **162,** 10–21 (2003).
13. Gomes, R., Levison, H. F., Tsiganis, K. & Morbidelli, A. Origin of the cataclysmic Late Heavy Bombardment period of the terrestrial planets. *Nature* **435,** 466–469 (2005).
14. Morbidelli, A., Brasser, R., Gomes, R., Levison, H. F. & Tsiganis, K. Evidence from the asteroid belt for a violent past evolution of Jupiter's orbit. *Astron. J.* **140,** 1391–1401 (2010).
15. Minton, D. A. & Malhotra, R. Dynamical erosion of the asteroid belt and implications for large impacts in the inner Solar System. *Icarus* **207,** 744–757 (2010).
16. Morbidelli, A. *et al.* Source regions and time scales for the delivery of water to Earth. *Meteorit. Planet. Sci.* **35,** 1309–1320 (2000).
17. Lécuyer, M., Gillet, P. & Robert, F. The hydrogen isotope composition of sea water and the global water cycle. *Chem. Geol.* **145,** 249–261 (1998).
18. Abe, Y., Ohtani, E., Okuchi, T., Righter, K. & Drake, M. in *Origin of the Earth and Moon* (eds Canup, R. M. & Righter, K.) 413–433 (Univ. Arizona Press, 2000).
19. Brownlee, D. *et al.* Comet 81P/Wild 2 under a microscope. *Science* **314,** 1711–1716 (2006).
20. Gounelle, M. *et al.* in *The Solar System Beyond Neptune* (eds Barucci, M. A. *et al.*) 525–541 (Univ. Arizona Press, 2008).
21. Ciesla, F. J. & Cuzzi, J. N. The evolution of the water distribution in a viscous protoplanetary disk. *Icarus* **181,** 178–204 (2006).
22. Butler, R. P. *et al.* Catalog of nearby exoplanets. *Astrophys. J.* **646,** 505–522 (2006).
23. Paardekooper, S. & Mellema, G. Halting type I planet migration in non-isothermal disks. *Astron. Astrophys.* **459,** L17–L20 (2006).
24. Paardekooper, S. & Papaloizou, J. C. B. On disc protoplanet interactions in a non-barotropic disc with thermal diffusion. *Astron. Astrophys.* **485,** 877–895 (2008).
25. Kley, W. & Crida, A. Migration of protoplanets in radiative discs. *Astron. Astrophys.* **487,** L9–L12 (2008).

26. Masset, F. S. & Casoli, J. On the horseshoe drag of a low-mass planet. II. Migration in adiabatic disks. *Astrophys. J.* **703,** 857–876 (2009).
27. Masset, F. S. & Papaloizou, J. C. B. Runaway migration and the formation of hot Jupiters. *Astrophys. J.* **588,** 494–508 (2003).
28. Morbidelli, A., Tsiganis, K., Crida, A., Levison, H. F. & Gomes, R. Dynamics of the giant planets of the Solar System in the gaseous protoplanetary disk and their relationship to the current orbital architecture. *Astron. J.* **134,** 1790–1798 (2007).
29. Batygin, K. & Brown, M. E. Early dynamical evolution of the Solar System: pinning down the initial conditions of the Nice model. *Astrophys. J.* **716,** 1323–1331 (2010).
30. Raymond, S. N., O'Brien, D. P., Morbidelli, A. & Kaib, N. A. Building the terrestrial planets: constrained accretion in the inner Solar System. *Icarus* **203,** 644–662 (2009).

Supplementary Information is linked to the online version of the paper at www.nature.com/nature.

Acknowledgements K.J.W. and A.M. were supported by the Helmholtz Alliances 'Planetary Evolution and Life' programme. S.N.R and A.M.M. were supported by the EPOV and PNP programmes of CNRS. D.P.O'B. was supported by the NASA PG&G programme. A.M.M. was also supported by the NASA post-doctoral programme and the Goddard Center for Astrobiology. We thank the Isaac Newton Institute DDP programme for hosting some of us at the initial stage of the project; we also thank J. Chambers for comments that improved the text. Computations were done on the CRIMSON Beowulf cluster at OCA.

Author Contributions K.J.W. managed the simulations and analysis and was the primary writer of the manuscript. A.M. initiated the project, updated and tested software, ran and analysed simulations, and wrote significant parts of the manuscript. S.N.R. helped initiate the project, advised on simulations and contributed substantially to the manuscript. D.P.O'B. helped initiate the project and assisted in writing. A.M.M. assisted in software updates and in writing.

Author Information Reprints and permissions information is available at www.nature.com/reprints. The authors declare no competing financial interests. Readers are welcome to comment on the online version of this article at www.nature.com/nature. Correspondence and requests for materials should be addressed to K.J.W. (kwalsh@boulder.swri.edu).